Contents lists available at SCCE

Journal of Soft Computing in Civil Engineering

Journal homepage: www.jsoftcivil.com

Evaluating Adaptive Neuro-Fuzzy Inference System (ANFIS) to Assess Liquefaction Potential and Settlements Using CPT Test Data

Himanshu Kumar Jangir[1*], Rupali Satavalekar[2]

1. Mtech Student, Dr. B.R. Ambedkar National Institute of Technology Jalandhar, Jalandhar, Punjab, India
2. Assistant Professor, Dr. B.R. Ambedkar National Institute of Technology Jalandhar, Jalandhar, Punjab, India
Corresponding author: *himanshujangir1995@gmail.com*

https://doi.org/10.22115/SCCE.2022.345237.1456

ARTICLE INFO

Article history:
Received: 01 June 2022
Revised: 02 August 2022
Accepted: 01 October 2022

Keywords:
Settlements;
Adaptive neuro-fuzzy inference system (ANFIS);
Liquefaction;
Liquefaction-potential;
Sub-clustering;
MATLAB.

ABSTRACT

Liquefaction occurs when saturated, non-cohesive soil loses strength. This phenomenon occurs as the water pressure in the pores rises and the effective stress drops because of dynamic loading. Liquefaction potential is a ratio for the factor of safety used to figure out if the soil can be liquefied, and liquefaction-induced settlements happen when the ground loses its ability to support construction due to liquefaction. Traditionally, empirical and semi-empirical methods have been used to predict liquefaction potential and settlements that are based on historical data. In this study, MATLAB's Fuzzy Tool Adaptive Neuro-Fuzzy Inference System (ANFIS) (sub-clustering) was used to predict liquefaction potential and liquefaction-induced settlements. Using Cone Penetration Test (CPT) data, two ANFIS models were made: one to predict liquefaction potential (LP-ANFIS) and the other to predict liquefaction-induced settlements (LIS-ANFIS). The RMSE correlation for the LP-ANFIS model (input parameters: Depth, Cone penetration, Sleeve Resistance, and Effective stress; output parameters: Liquefaction Potential) and the LIS-ANFIS model (input parameters: Depth, Cone penetration, Sleeve Resistance, and Effective stress; output parameters: Settlements) was 0.0140764 and 0.00393882 respectively. The Coefficient of Determination (R2) for both the models was 0.9892 and 0.9997 respectively. Using the ANFIS 3D-Surface Diagrams were plotted to show the correlation between the CPT test parameters, the liquefaction potential, and the liquefaction-induced settlements. The ANFIS model results displayed that the considered soft computing techniques have good capabilities to determine liquefaction potential and liquefaction-induced settlements using CPT data.

How to cite this article: Jangir HK, Satavalekar R. Evaluating adaptive neuro-fuzzy inference system (ANFIS) to assess liquefaction potential and settlements using CPT test data. J Soft Comput Civ Eng 2022;6(3):119–139. https://doi.org/10.22115/scce.2022.345237.1456

2588-2872/ © 2022 The Authors. Published by Pouyan Press.
This is an open access article under the CC BY license (http://creativecommons.org/licenses/by/4.0/).

1. Introduction

In many parts of the world, a serious threat during earthquakes occurs as a result of the liquefaction of granular soil in a saturated and loose state. Due to liquefaction, ground deformations occur, which caused severe damage to the lifeline of designed structures during earthquakes. The most common types of deformation are lateral spread and ground settlement, which has caused by liquefaction [1]. Geotechnical earthquake engineering has been disadvantageous to the challenge of liquefaction potential and liquefaction-induced settlements that are associated with several phenomena, including loss of re-edification of the ground due to the liquefied soil escape (sand boils), bearing capacity failures, soil-structure interaction ratcheting, lateral spreading under zero volume change, and liquefied soil. Under liquefaction, loose granular soil is compacted and densified, resulting in horizontal settlements of surficial soil layers due to vertical deformation induced by liquefaction [2].

In numerical analysis, earthquake-induced liquefaction can be understood as a 1-D phenomenon in which an increase in pore pressure is caused due to earthquake-induced cyclic shear and compressive forces in the free field, thereby reducing the stability of the soil. When water flow is used to dissipate the excess pore pressure (u), it results in the resolidification of the soil due to the vertical settlements of the ground surface after liquefaction. In situations where liquefaction might result in significant damage, the complexity of analyzing and obtaining high-quality samples of loose sandy soil can limit the use of samples. An analytical method, numerical method, field testing, and laboratory testing are a variety of methods that are used for the liquefaction potential and the liquefaction-induced ground settlements calculation, including the combination of the two methods. Semi-empirical techniques based on field test data for estimating liquefaction potential and liquefaction-induced settlements are most appropriate for prediction and for providing preliminary estimates for higher-risk projects and low-to medium-risk projects [3].

Soils are complex and ambiguous in general, resulting in incoherent composition, inaccuracies in soil sampling, boring, characterization, field testing, laboratory testing, and uncertainty [4]. Artificial intelligence (AI) outperforms traditional approaches in terms of prediction capability, resulting in AI's simplicity of use in modeling and the complex behavior of most geotechnical materials and phenomena. The capacity of AI to handle several outputs, as opposed to a regression model that can only manage one, is its primary advantage over regression modeling. Another significant benefit is that they do not rely on basic assumptions like linear behavior, making them perfect for modeling materials with a wide range of properties and complexity, such as soils and rocks. Because neural networks are strong generalizers, capable of approximating universal functions, being resistant to noisy or missing data, and accommodating numerous nonlinear variables, they can describe complicated mechanical phenomena [5].

Researchers found the neuro-fuzzy technique suited for liquefaction potential assessment, and the models exhibited high agreement with current findings and prediction abilities. Rahman et al. [6] employed a neuro-fuzzy network to predict liquefaction potential. Kayadelen et al. [7] compare GEP and ANFIS findings for liquefaction potential and find significant agreement with

the results. Ramakrishnan et al. [8] employed ANN to assess liquefaction probability using 2001 Bhuj earthquake data, Gujarat, India. Xue et al. [9] created an ANFIS model for anticipating liquefaction potential, and the results were promising. Kumar et al. [10] designed a neural network model for liquefaction potential using SPT data. Karkh et al. [11] utilized SPT-N data from coastal areas of Allahabad (India) to create a neuro-fuzzy model for the prediction of liquefaction potential. Sharafi et al. [12] created a backpropagation neural network approach to predict CRR. Kumar et al. [13] employed ANFIS and ANN to estimate liquefaction potential and concluded additional datasets for training, testing, and validation might enhance confidence and reliability. All of the models' correlation coefficients are within acceptable bounds, demonstrating that neuro-fuzzy models may make reliable predictions.

For the prediction of liquefaction potential and liquefaction-induced settlements empirical and semi-empirical methods have been used that are based on historical data. These methods follow non-linear relations between parameters which are determined in the field by using CPT, SPT, CPTu, and SCPTu test methods. CPT test is a widely acceptable and reliable field test in the geotechnical field. Few studies are available on the analysis or prediction of liquefaction-induced settlements using ANFIS model analysis. The objective of the study is to develop an ANFIS model for the determination of liquefaction potential and liquefaction-induced settlements using CPT test data by using only basic parameters which were obtained by field test and determining the correlation between these parameters and liquefaction potential and liquefaction-induced settlements because ANFIS models also follow the non-linear analysis.

2. Research significance

Many factors are taken into account while calculating liquefaction potential and liquefaction-induced settlements, as well as multiple difficult analytical and numerical processes. In most circumstances, however, getting such characteristics in the field is not feasible since part of the essential data may not be accessible. Therefore, it is necessary to develop a simple prediction model that can be easily collected from a database of field observations and depends only on a few factors. Consequently, to predict liquefaction potential and liquefaction-induced settlements, this research aims to offer a tool that can be used for the prediction that may occur after an earthquake occurs.

3. Computation of liquefaction potential and liquefaction-induced settlements

For determining Liquefaction-Induced Settlements first Liquefaction potential is needed to calculate which is determined by using Idriss and Boulanger [14] method and for determining Liquefaction-Induced Settlements a new probabilistic approach was used which was developed by Juang et al. [7].

3.1. Computation of liquefaction potential using idriss and boulanger method

For determining the liquefaction potential of soil Idriss and Boulanger [14] developed a semi-empirical method using Youd et al. [15] determined equation of cyclic resistance ratio (CRR). The steps used for the calculation of liquefaction-induced settlements are as follows

• The cyclic stress ratio (CSR) calculation.

• The soil's cyclic resistance ratio (CRR) calculation.

• The Liquefaction Potential calculation.

• The Liquefaction-Induced Settlements calculation.

3.1.1. Using CPT data calculation of cyclic stress ratio (CSR)

Using the maximum vertical stress cyclic stress ratio (CSR) is determined by using Eq. (1)

$$\mathrm{CSR}_{\mathrm{M}\sigma'_{\mathrm{v}}} = \quad 0.65\left(\frac{\sigma_{\mathrm{v}}}{\sigma'_{\mathrm{v}}}\right)\left(\frac{a_{\max}}{\mathrm{g}}\right)\mathrm{r_d} \tag{1}$$

Where σ_{v}= total vertical stress; $\mathrm{CSR}_{\mathrm{M}\sigma'_{\mathrm{v}}}$ = cyclic stress ratio for specific earthquake magnitude and in-situ vertical effective stress; g = gravitational acceleration; σ'_{v} = effective vertical stress; $\mathrm{r_d}$= stress reduction coefficient $a_{\max}$ = peak horizontal ground acceleration.

Using the following equations the average value of the stress reduction coefficient $\mathrm{r_d}$ can be estimated:

$$\mathrm{r_d} = 1.0 - 0.00765\mathrm{Z} \ \ (\mathrm{Z} \leq 9.15\mathrm{m}) \tag{2}$$

$$\mathrm{r_d} = 1.174 - 0.0267\mathrm{Z} \ \ (9.15\mathrm{m} < \mathrm{Z} \leq 23\mathrm{m}) \tag{3}$$

$$\mathrm{r_d} = 0.744 - 0.008\mathrm{Z} \ \ (23\mathrm{m} < \mathrm{Z} \leq 30\mathrm{m}) \tag{4}$$

$$\mathrm{r_d} = 0.50\mathrm{Z} \quad (\mathrm{Z} > 30\mathrm{m}) \tag{5}$$

3.1.2. Using CPT data calculation of cyclic resistance ratio (CRR)

Depending on the normalized cone resistance the $CRR_{7.5}$ is then calculated using the following equations [15].

If $Q_{ctN} < 50$

$$\mathrm{CRR}_{7.5} = 0.833\left[\frac{\mathrm{Q_{ctN}}}{1000}\right] + 0.05 \tag{6}$$

If $50 < Q_{ctN} < 160$

$$\mathrm{CRR}_{7.5} = 93\left[\frac{\mathrm{Q_{ctN}}}{1000}\right]^3 + 0.08 \tag{7}$$

Where $CRR_{7.5}$ = cyclic resistance ratio for an equivalent magnitude of 7.5 events; Q_{ctN}= normalized sand penetration resistance.

The *CPT* tip resistance (q_{c1N}) is normalized as follows

$$Q_{ctN}=(\frac{P_a}{\sigma'_v})^n(\frac{q_t}{P_a}) \quad (8)$$

Where q_t = cone tip resistance; Pa = atmospheric pressure; n = stress exponent

For the stress exponent, n Robertson [1] provides a function as shown in Eq. (9)

$$\mathrm{n} = 0.381(Ic) + 0.05\left(\frac{\sigma'_\mathrm{v}}{\mathrm{P_a}}\right) - 0.15 \quad \leq 1.0 \quad (9)$$

Where Ic= Soil behavior index

$$Ic = [(3.47 - \log(\mathrm{Q_{ctN}}))^2 + (\log(\mathrm{F}) + 1.22)^2]^{0.5} \quad (10)$$

F = normalized friction ratio; Q_{ctN} = normalized cone tip resistance and F is determined as follows:

$$\mathrm{F} = \frac{\mathrm{f_s}}{(\mathrm{q_t})} \times 100\% \quad (11)$$

Where *f*s = sleeve friction; q_t= cone tip resistance;

3.1.3. The Liquefaction Potential

Using *CPT* results the factor of safety against liquefaction is calculated and is performed using the fines content correlations [16] by using Eq. (12) as

$$\mathrm{FS} = (\frac{\mathrm{CRR_{7.5}}}{\mathrm{CSR}}) \times \mathrm{MSF} \times \mathrm{K_\sigma} \times \mathrm{K_\alpha} \quad (12)$$

Where *FS* = factor of safety against liquefaction; CSR = cyclic stress ratio for a given magnitude; K_σ = overburden correction factor; $CRR_{7.5}$ = cyclic resistance ratio for an equivalent magnitude of 7.5 events; MSF = magnitude scaling factor; K_α = correction factor for sloping ground, assumed to be equal to one for level ground.

The magnitude scaling factor, MSF, can be calculated in a variety of methods, according to the relative density and overburden stress are used to calculate the overburden correction factor, K_σ, which can be calculated by using Eq. (13)

$$\mathrm{K_\sigma} = \left(\frac{\sigma'_\mathrm{v}}{\mathrm{P_a}}\right)^{\mathrm{f-1}} \quad (13)$$

Where f = empirical exponent; depends on relative density.

3.2. Computation of liquefaction-induced settlements using Juang *et al.* [17] probabilistic method

3.2.1. Volumetric strain

According to Juang et al. [17], the settlement amount is usually listed as a range due to the nature of case histories, to estimate the possibility of exceeding a specified settlement amount [17]. A probabilistic method was developed by Juang et al. [17] to address this problem based on

Ishihara and Yoshimine et al. [18] method. To develop the proposed method, Liquefaction Potential, liquefaction probability, and maximum likelihood concepts were utilized.

To define the relationships between volumetric strains, ε_v, Q_{ctN} and FS Juang et al. [17] used Ishihara and Yoshimine's formulae with the following equations

$$\varepsilon_v = 0 \qquad for \qquad (FS \geq 2) \tag{14}$$

$$\varepsilon_v = \text{Min} \quad \frac{a_0 + a_1 \ln(Q_{ctN})}{\frac{1}{(2-FS)} - [a_2 + a_3 \ln(Q_{ctN})]} \; for \; \left(2 - \frac{1}{[a_2 + a_3 \ln(Q_{ctN})]} < FS < 2\right) \tag{15}$$

$$\varepsilon_v = b_0 + b_1 \ln(Q_{ctN}) + b_2 \ln(Q_{ctN})^2 \quad for \; \left(FS \leq 2 - \frac{1}{[a_2 + a_3 \ln(Q_{ctN})]}\right) \tag{16}$$

3.2.2. Liquefaction-induced settlements

Juang et al. [17] proposed an equation for the determination of total liquefaction-induced settlements as shown in Eq. (17)

$$Sp = M\Sigma_{i=1}^{r} \varepsilon_v \Delta z_i \tag{17}$$

Where ε_v volumetric strain for the ith layer, Δz_i is the ith layer's thickness, M represents a modal bias correction factor and N is the number of layers. The calculation process is demonstrated by the flow chart as shown in Fig. 1.

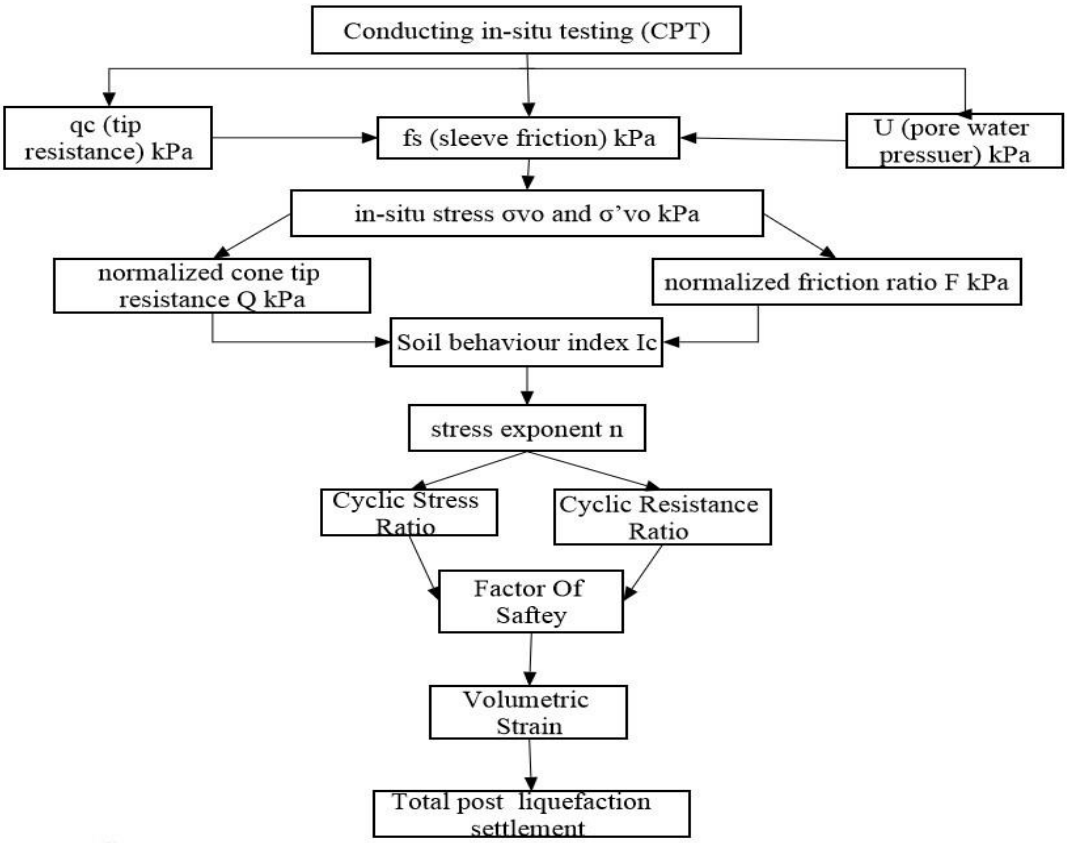

Fig. 1. Flowchart of Calculating process for Total Liquefaction-Induced Settlements.

4. Dataset

Cone penetration tests (*CPT*) were conducted by Premstaller Geotechnik ZT GmbH [19] across Germany and Austria, and the findings are included in this dataset. These cone penetration tests were conducted using core drilling as part of the processing procedure, and they were placed within a maximum depth of 50 m based on grain size distribution from the in-situ testing, allowing in-situ data to be interpreted. It also offers a structure for merging in-situ measurements (q_c, fs). As shown in Table 1 and Table 2 datasets were used for modeling of the liquefaction potential (LP-ANFIS) model and liquefaction-induced settlements (LIS-ANFIS) model respectively, and according to depth the variation of parameters determined by using the *CPT* test are shown in Fig. 1.

Table 1
Dataset Used for Modelling for LP-ANFIS model.

S.N.	Depth (m)	Cone resistance qc (kPa)	Sleeve Resistance fs (kPa)	Effective stress σ'_v (kPa)	Liquefaction Potential
1.	15.28	2600	38	140.42	0.036131
2.	14.44	1450	29	132.7	0.021774
3.	3.72	3650	14	34.19	0.353585
4.	16.36	4000	40	150.35	0.06383
5.	15.26	2550	38	140.24	0.035564
6.	5.26	3300	9	48.34	0.390718
7.	10.48	2700	33	96.31	0.055554
8.	3.68	3550	11	33.82	0.430503
9.	11.14	2550	27	102.38	0.059889
10.	10.1	3350	27	92.82	0.092406
11.	14.36	1300	28	131.97	0.019375
12.	9.74	3850	23	89.51	0.136071
13.	0.48	4550	48	4.41	0.418725
14.	14.2	1250	27	130.5	0.01926
15.	9.34	5100	8	85.83	0.625867
16.	10.96	2800	24	100.72	0.077037
17.	17.68	2600	36	162.48	0.035537
18.	8	3500	8	73.52	0.229479
19.	13	1400	25	119.47	0.025526
20.	16.98	2750	36	156.05	0.03865
21.	-	-	-	-	-
955.	4.12	3450	4	37.86	1.027124

Table 2
Dataset Used for Modelling for LIS-ANFIS MODEL.

S.N.	Depth (m)	Cone resistance qc (kPa)	Sleeve Resistance f_s (KPa)	Effective stress σ'_v (KPa)	Liquefaction Potential	Liquefaction -Induced Settlements (mm)
1.	15.28	2600	38	140.42	0.036131	0.66466311
2.	14.44	1450	29	132.7	0.021774	1.06321442
3.	3.72	3650	14	34.19	0.353585	0.14358409
4.	16.36	4000	40	150.35	0.06383	0.43598614
5.	15.26	2550	38	140.24	0.035564	0.67551647
6.	5.26	3300	9	48.34	0.390718	0.1680113
7.	10.48	2700	33	96.31	0.055554	0.5052231
8.	3.68	3550	11	33.82	0.430503	0.13243897
9.	11.14	2550	27	102.38	0.059889	0.52661216
10.	10.1	3350	27	92.82	0.092406	0.37114475
11.	14.36	1300	28	131.97	0.019375	1.16404509
12.	9.74	3850	23	89.51	0.136071	0.29223309
13.	0.48	4550	48	4.41	0.418725	0.04669002
14.	14.2	1250	27	130.5	0.01926	1.18917452
15.	9.34	5100	8	85.83	0.625867	0.11027778
16.	10.96	2800	24	100.72	0.077037	0.45782537
17.	17.68	2600	36	162.48	0.035537	0.70520842
18.	8	3500	8	73.52	0.229479	0.24064562
19.	13	1400	25	119.47	0.025526	1.00823765
20.	16.98	2750	36	156.05	0.03865	0.65391614
21.	-	-	-	-	-	-
955.	4.12	3450	4	37.86	1.027124	0.07164265

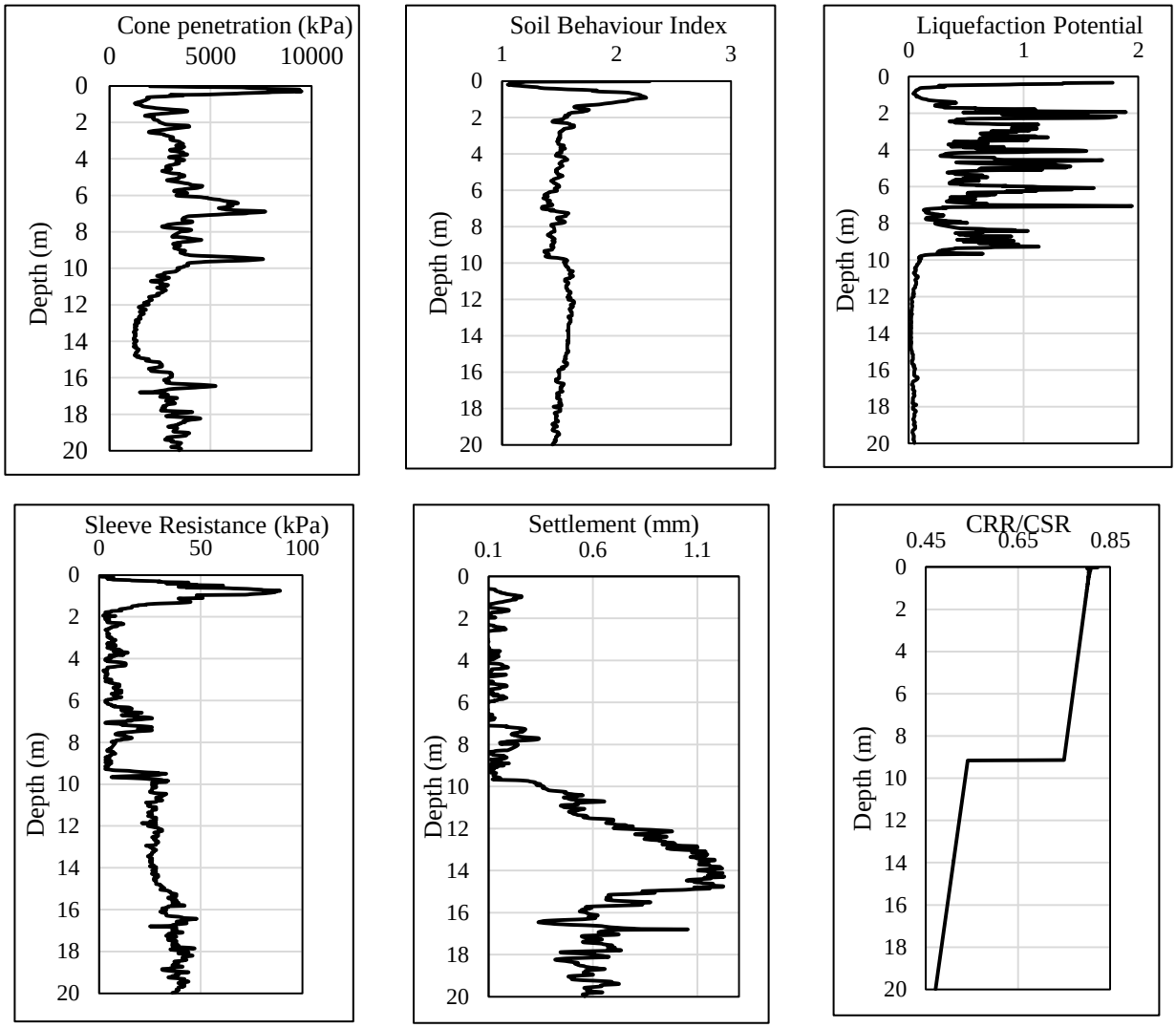

Fig. 2. The graph between Depth and Various Parameters measured by the CPT test.

4.1. Preprocessing of dataset for model development

Datasets are used in AI-based computing and statistical regression models. Thus, data preparation difficulties must be considered for more accurate models. Normalization methods may be used to scale data, an accurate model depends on correlations between independent input variables, outputs variables, data scales, and variable distributions. Data normalization adjusts numbers on disparate scales to a single scale and it speeds up machine learning algorithm training when input data ranges are vast. Normalizing or standardizing contributes to avoiding local optima or unaltered outcomes and by standardizing features, data variations can be reduced [20]. Feature scaling methods were used for the normalization of data, this strategy limits the dataset's values to arbitrary values a and b. The formula for normalization of raw data to range of $[a, b]$ shown in Eq. 18.

$$X_n = a + (a - b)\frac{X_{min} - X}{X_{max} - X_{min}} \tag{18}$$

Where X_{max}, X_{min}, and X_n are the maximum, minimum, and normalized values of the variable, and a = 0.05 and b = 0.95 are considered in Eq. (18).

5. Overview of the ANFIS

5.1. ANFIS's fundamental concept

An adaptive neuro-fuzzy inference system (ANFIS) was developed based on the Takagi-Sugeno fuzzy inference system, which is another type of artificial neural network. This method was created in the early 1990s and it combines fuzzy logic and neural network advantages in one framework. ANFIS was designed to be a multipurpose estimator, and machine learning is used to help ANFIS for approximate nonlinear functions through fuzzy IF-THEN rules. The best parameters produced using a genetic algorithm can be used to make ANFIS more efficient and optimum [21].

5.2. ANFIS architecture as a mathematical representation

ANFIS uses a hybrid learning approach to build input-output maps that combine neural networks and fuzzy rule knowledge. ANFIS builds input-output mappings as it follows adaptable neural networks by specified input-output data pairings and If-Then rules for neural networks, using x_1 and x_2 as inputs, y as output, A_i and A_n^2 as input membership functions, and w_i and w_n^2 as rule firing strengths, as shown in Fig. 3. To execute the fuzzy inference procedure, ANFIS employs five network layers [22].

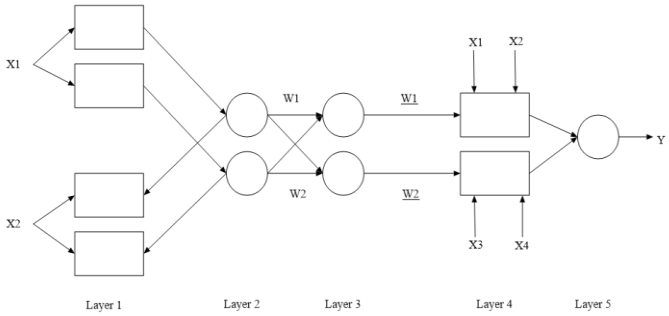

Fig. 3. The ANFIS structure [23].

ANFIS comprises five interconnected layers: input, base, intermediate, result, and output. There are membership functions associated with each node. The structure of the data is determined by input data, membership function degree, input and output membership rules, and functions. In addition to having strong training, construction, and classification capabilities ANFIS utilizes neural network learning methods and fuzzy logic. By changing membership function degree, the allowable error change depending on parameters so during training output values get closer to real values. Its learning mechanism uses an error propagation approach to minimize the root mean square error (RMSE) between the network output and real output value. Since this system employs 0 and 1-degree Sugeno fuzzy models, its output membership function comprises only constant and linear functions. Using a trial and error process determination of the best membership function and degree of membership can be done as ANFIS is a membership functions network. The network performance is assessed using test data, if test data assessment

criteria are not approved, the degree of membership function can raise, after network training and testing are repeated. Finally, the top network is chosen among the best networks for distinct membership functions [24].

5.3. Sub-clustering

Sub-clustering combines unsupervised data by assessing space potential features. It may be used to estimate the number of clusters and cluster centers for a given dataset when there is no clear concept. Data points are evaluated as cluster centers by subtractive clustering based on the density surrounding them. Data points that are close to the cluster center lose potential because of being chosen as the initial cluster center. A cluster center is then determined, and then those data points surrounding it are removed. Cluster radius is a cluster's effect in several data dimensions, this influence radius determines the cluster count. A narrower radius leads to smaller data clusters, which results in more rules. Choosing the right influence radius for data clustering is crucial [25].

6. Modelling process of ANFIS

6.1. LP-ANFIS model

The dataset used to train the LP-ANFIS model is provided in **Error! Reference source not found.**, and the input parameter from the dataset was separated into two parts: testing data (30%) and training data (70%). The sub-clustering parameters were (i) reject ratio = 0.15, (ii) acceptability ratio = 0.5, (iii) squash factor = 1.25, and (iv) range of influence = 0.01. The parameters of the ANFIS model are as follows: number of nonlinear parameters = 360; total number of parameters = 585; number of training data pairs = 677; number of nodes = 457; number of checking data pairs = 0; number of fuzzy rules = 45 and number of linear parameters = 225 as shown in Fig. 4 and structure of the five-layer network for LP-ANFIS is presented in Fig. 5 (a)-(b) which uses the testing and training subsets of the dataset the model was trained (RMSE = 0.0140764). By plotting a scatter plot graph between the liquefaction potential calculated results and LP-ANFIS model training dataset results, the obtained R^2 value is 0.9953, which is in good agreement as shown in Fig. 6.

```
Start training ANFIS ...

1    0.0140764
2    0.0162825

Designated epoch number reached. ANFIS training completed at epoch 2.

Minimal training RMSE = 0.0140764

ANFIS info:
    Number of nodes: 457
    Number of linear parameters: 225
    Number of nonlinear parameters: 360
    Total number of parameters: 585
    Number of training data pairs: 677
    Number of checking data pairs: 0
    Number of fuzzy rules: 45
```

Fig. 4. LP-ANFIS model Training set parameter.

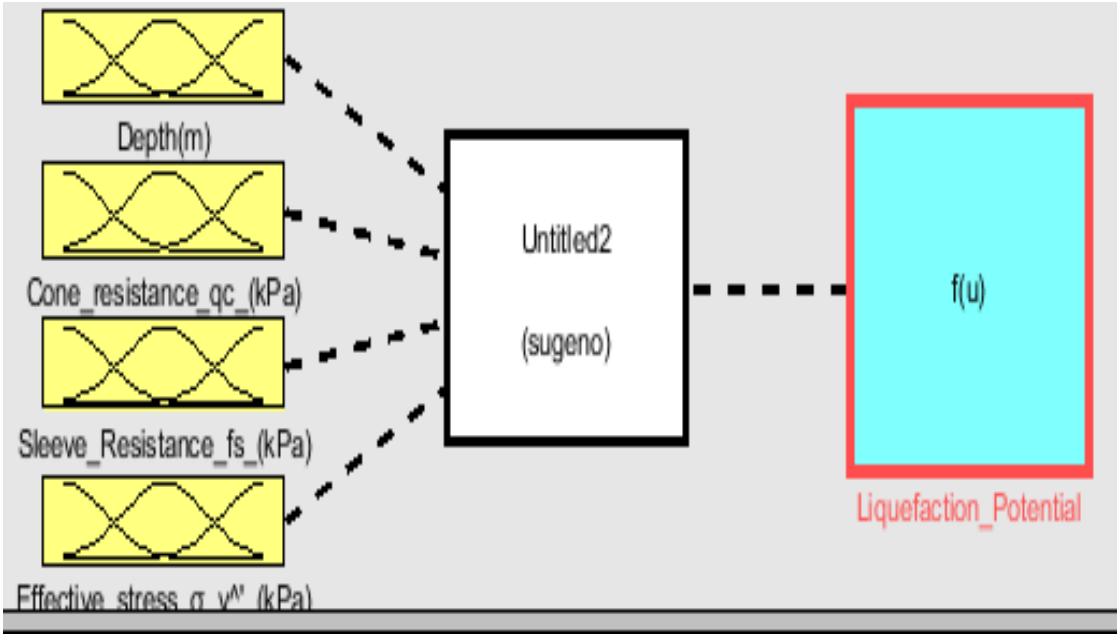

(a)

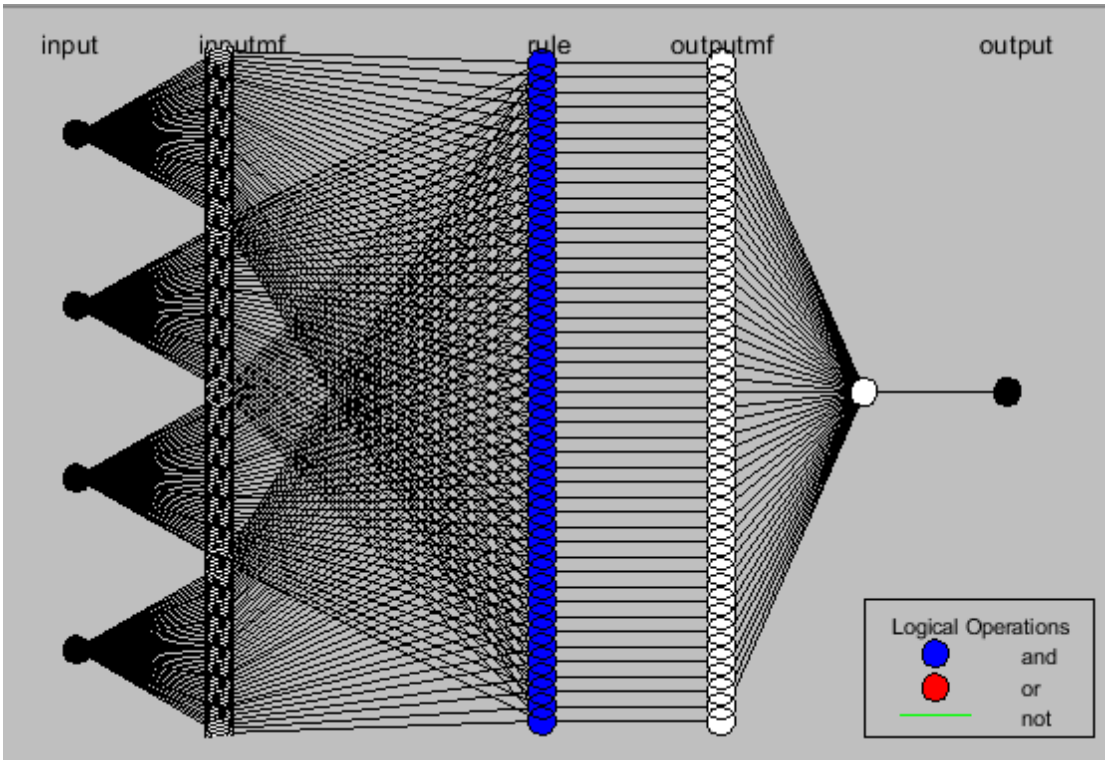

(b)

Fig. 5. LP-ANFIS model structure.

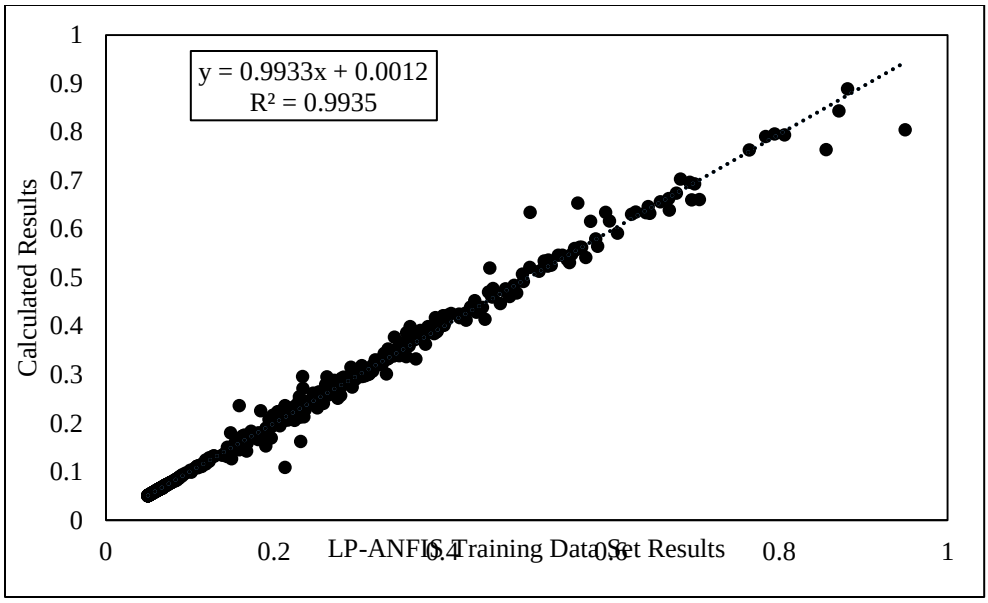

Fig. 6. Scatter Plot Graph between Liquefaction Potential of Calculated results and LP-ANFIS model training dataset results.

6.1.1. Validation of LP-ANFIS model

For validation of the results of the LP-ANFIS model training, the RMSE for the testing dataset attained was 0.026302 and by plotting a scatter plot graph between the liquefaction potential calculated results and LP-ANFIS model testing dataset results, the obtained R^2 value is 0.9804, which is in good agreement as shown in Fig. 7.

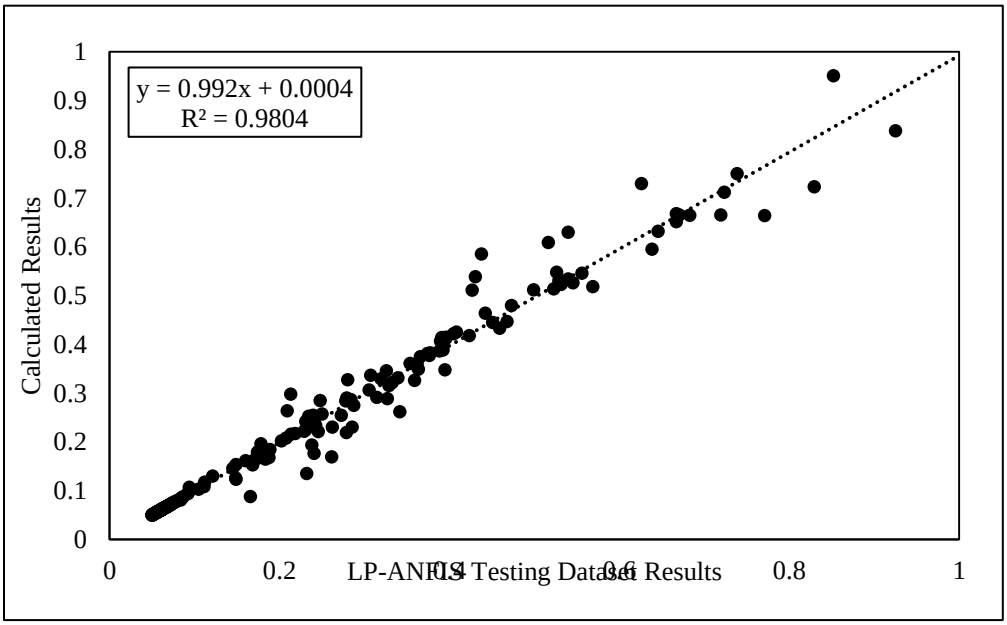

Fig. 7. Scatter Plot Graph between Liquefaction Potential calculated results and LP-ANFIS model testing dataset results.

6.2. LIS-ANFIS model

The dataset used to train the LIS-ANFIS model is provided inTable 2, and the input parameter dataset was separated into two parts: testing data (30%) and training data (70%). The sub-clustering parameters were (i) reject ratio = 0.15, (ii) acceptability ratio = 0.5, (iii) squash factor = 1.25, and (iv) range of influence = 0.01. The parameters of the ANFIS model are as follows: number of nonlinear parameters = 410; total number of parameters = 656; number of training data pairs = 667; number of nodes = 500; number of checking data pairs = 0; number of fuzzy rules = 41 and number of linear parameters = 246 as shown in Fig. 8. The structure of five-layers LIS-ANFIS model is illustrated in Fig. 9 (a)-(b) which is achieved using the testing and training subsets of the dataset the model was trained (RMSE was 0.00393882). By plotting a scatter plot graph between the liquefaction-induced settlements of calculated results and LIS-ANFIS model training dataset results, the obtained R^2 value is 0.9998, which is in good agreement as shown in Fig. 10.

```
Start training ANFIS ...

1    0.00393882
2    NaN

Designated epoch number reached. ANFIS training completed at epoch 2.

Minimal training RMSE = 0.00393882

ANFIS info:
    Number of nodes: 500
    Number of linear parameters: 246
    Number of nonlinear parameters: 410
    Total number of parameters: 656
    Number of training data pairs: 667
    Number of checking data pairs: 0
    Number of fuzzy rules: 41
```

Fig. 8. LIS-ANFIS model Training set parameter.

6.2.1. LIS-ANFIS model validation

For validation of the results of the LIS-ANFIS model training, the RMSE for the testing dataset obtained was 0.0052768 and by plotting a scatter plot graph between the liquefaction-induced settlements calculated results and LIS-ANFIS model training dataset results, the obtained R^2 value is 0.9996, which is in good agreement as shown in Fig. 11.

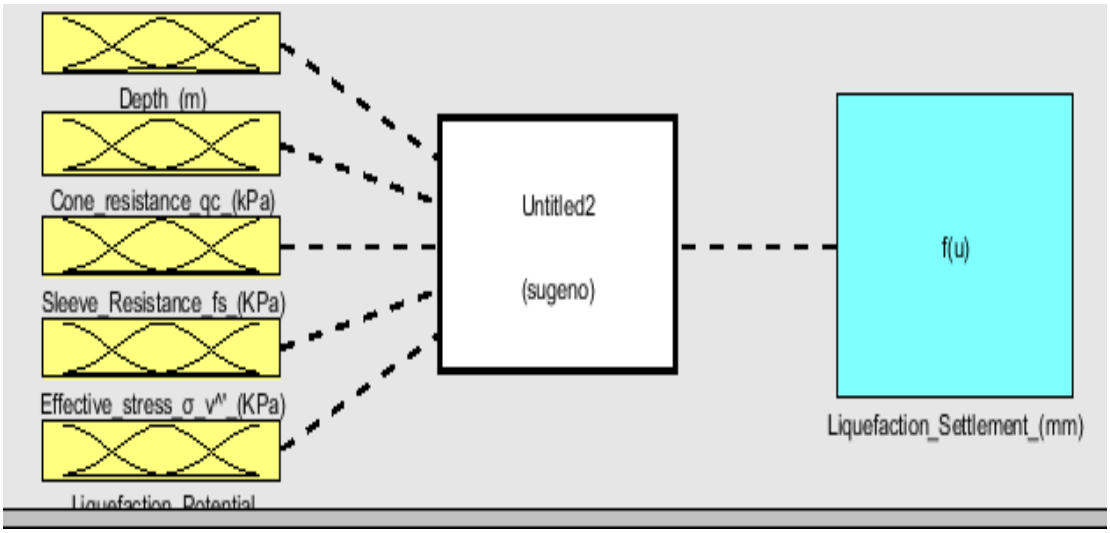

(a)

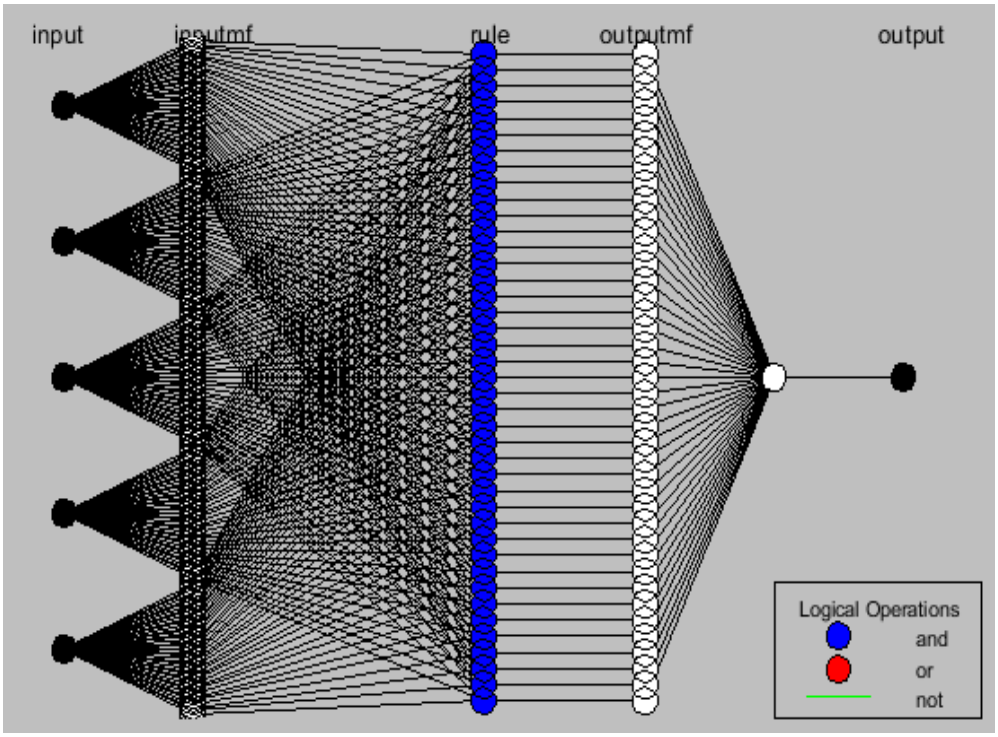

(b)

Fig. 9. LIS-ANFIS model structure.

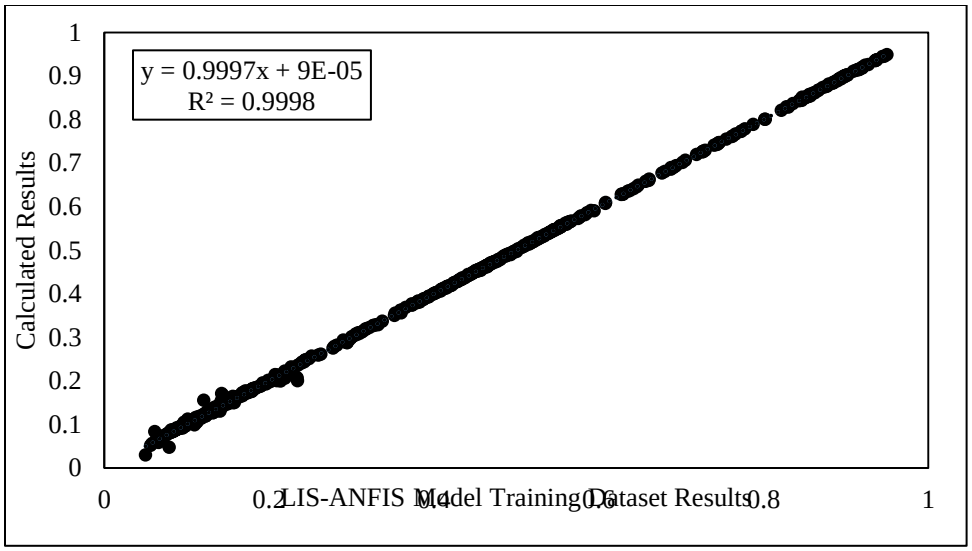

Fig. 10. Scatter Plot Graph between Liquefaction-induces settlements calculated results and LIS-ANFIS model training dataset results.

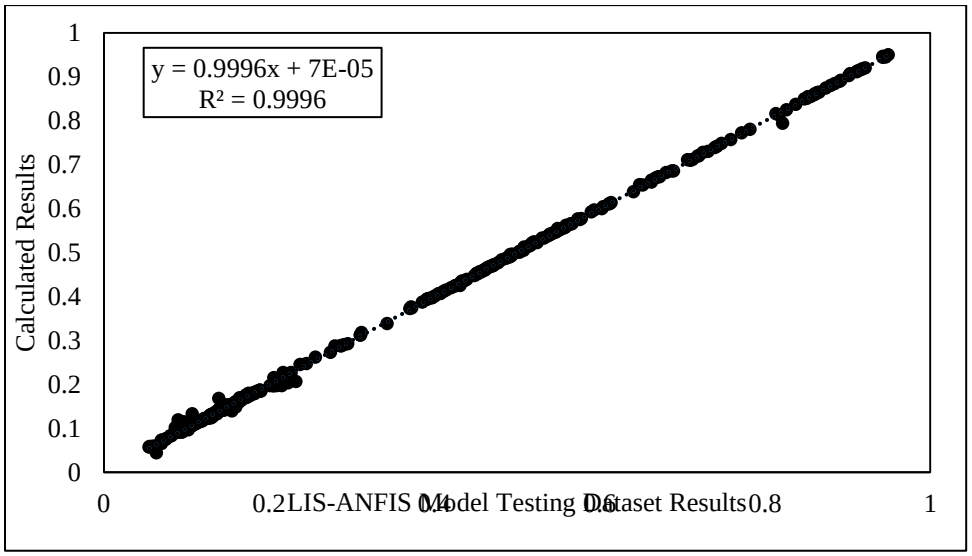

Fig. 11. Scatter Plot Graph between Liquefaction-induced settlements calculated results and LIS-ANFIS model testing dataset results

7. Results and discussion

7.1. ANFIS rule viewer

The ANFIS model can be visually employed using the rule viewer window, as shown in Fig. 12 and Fig. 13, the Rule Viewer displays fuzzy system inference. These are popular if-else rules that connect variables. This panel allows the user to graphically alter inputs using sliders to obtain the required outputs immediately. The commands were typed into the command field on the bottom left side of the display. Using this alteration in input values, observation of each fuzzy rule's output, the aggregated fuzzy set, and the defuzzified result can be done to examine the inference

process, which defines the fuzzy inference system input variables, output variables, membership functions, and fuzzy rules.

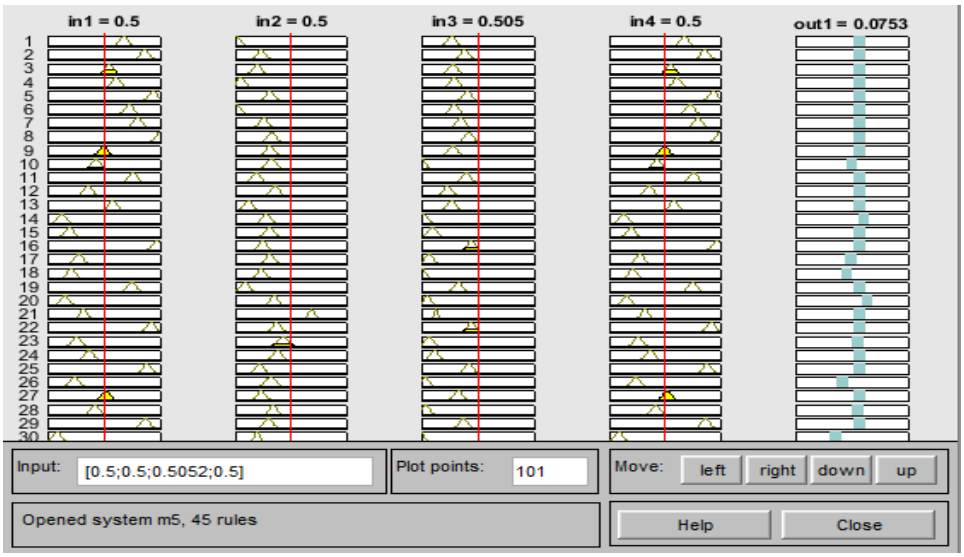

Fig. 12. LP-ANFIS model Rule viewer.

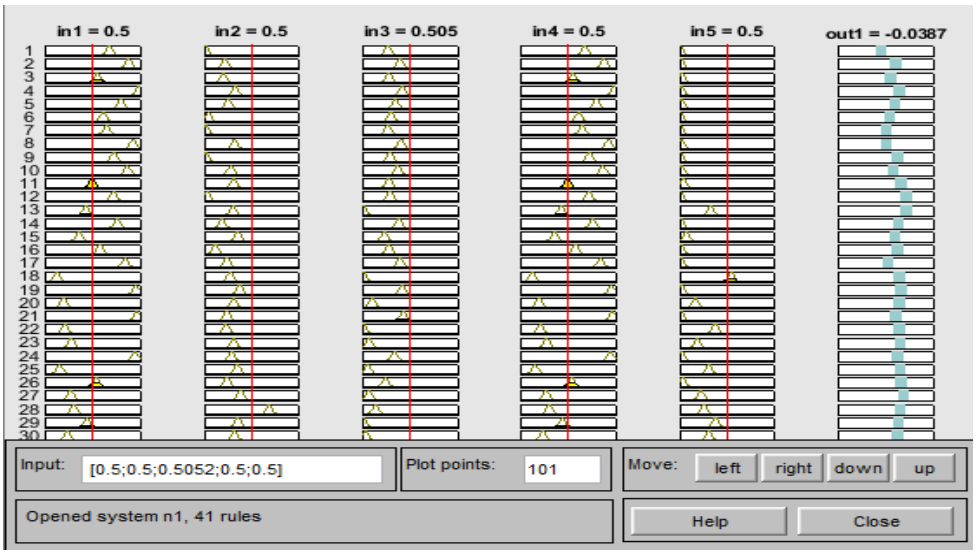

Fig. 13. LIS-ANFIS model Rule viewer.

7.2. ANFIS 3D-surface diagrams

The surface diagrams for "Sleeve resistance/Cone Penetration and Liquefaction Potential," and "Cone resistance/Effective Stress and Liquefaction Potential" are demonstrated in Fig. 14(a)-(b), and “Sleeve resistance/Cone Penetration and Liquefaction-Induced Settlements” and "Depth/ Liquefaction Potential and Liquefaction-Induced Settlements" are demonstrated in Fig. 15(a)-(b). These graphs represent the correlation between various factors that affect liquefaction potential and liquefaction-induced settlements.

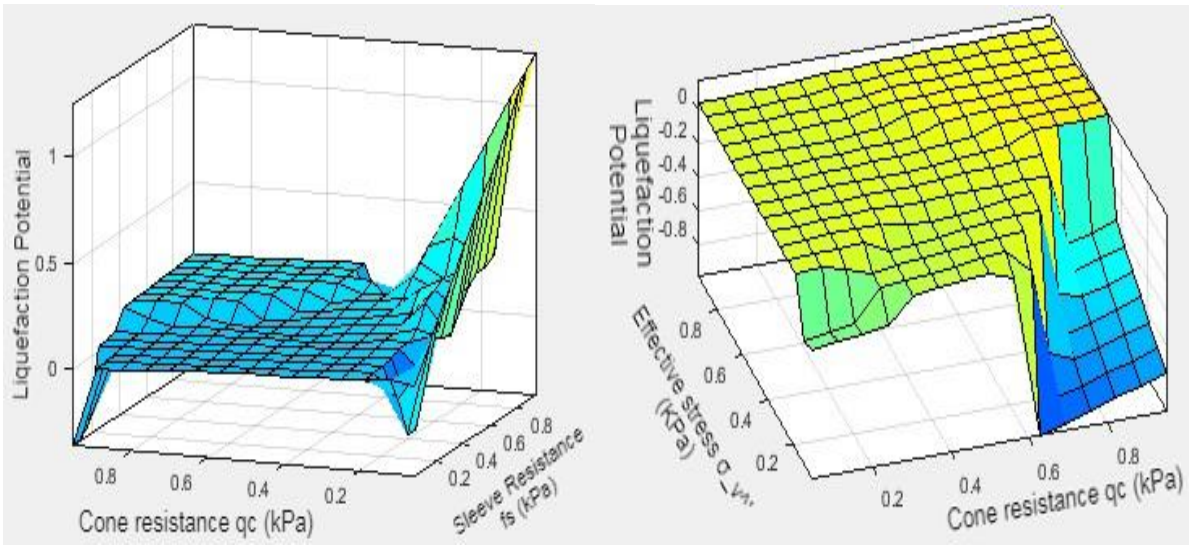

(a) (b)

Fig. 14. 3D-Surface Diagram from LP-ANFIS model between Liquefaction Potential and (a) Sleeve Resistance, Cone Penetration (b) Effective Stress, Cone Penetration.

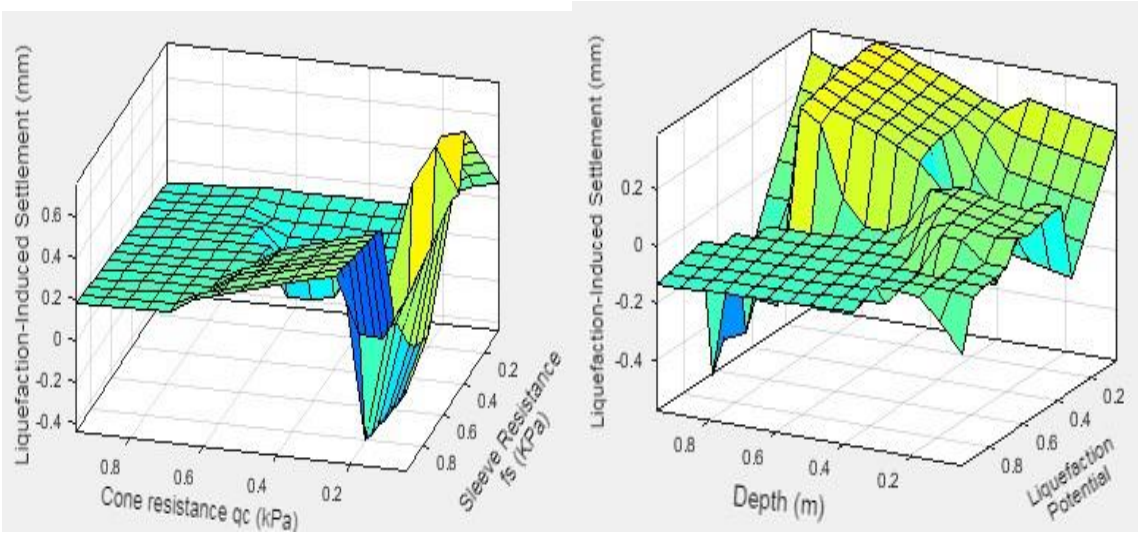

(a) (b)

Fig. 15. 3D-Surface Diagram from LIS-ANFIS model between Post Liquefaction Settlements and (a) Sleeve Resistance, Cone Penetration (b) Liquefaction Potential, Depth.

7.3. Comparison of calculated results and ANFIS results

The output of the ANFIS model was saved in a variable named result using the following command:

resultoutput = evalfis(input,result);

After producing output results from the LP-ANFIS model and LIS-ANFIS model, the coefficient of determination (R^2) between computed results and the entire data set results used for the ANFIS model was analyzed. Fig. 16 shows that the R^2 value for the LP-ANFIS model between

calculated results and results obtained from the complete dataset using the ANFIS model is 0.9892. Fig. 17 shows that the R^2 value for the LIS-ANFIS model between calculated results and results obtained from the complete dataset using the ANFIS model is 0.9997.

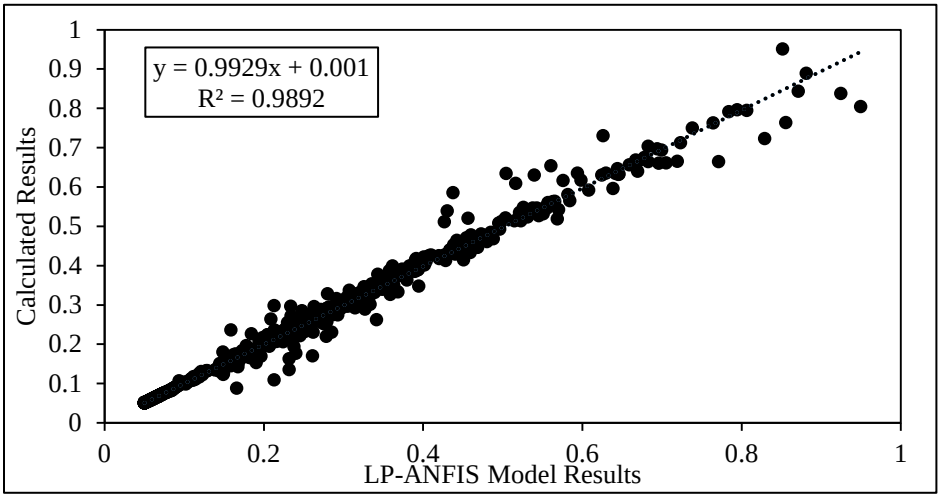

Fig. 16. Scatter Plot Graph between Liquefaction Potential calculated results and LP-ANFIS model results.

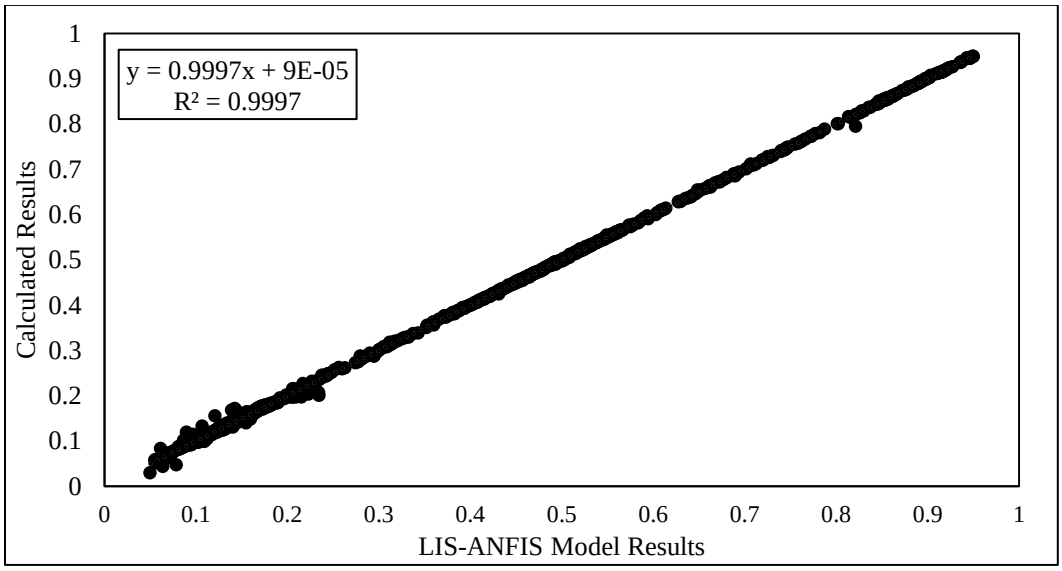

Fig. 17. Scatter plot graph between the liquefaction-induced settlements calculated results and LIS-ANFIS model results.

8. Conclusion

This research emphasizes the use of ANFIS to construct models for liquefaction potential and liquefaction-induced settlements. Because soil varies in composition and includes a vast number of components that impact liquefaction potential and settlements, estimating liquefaction potential and settlements in geotechnical engineering is a complex process. Fuzzy logic deals with the inaccuracy of system parameters, whereas neural networks deal with the underlying system's complexity and nonlinearity. The ANFIS models, which are presented in this work, are

easier to use and produce more accurate results in determining liquefaction potential than traditional empirical methodologies.

The following are the results from the investigation:

The LP-ANFIS model training error is 0.01400764 and the validation error is 0.026302, respectively, while the LIS-ANFIS model training error is 0.00393882 and the validation error is 0.0052768, and it can be concluded that the findings are in excellent agreement with the original results. The ANFIS model results were verified in Excel using a scatter plot graph between complete dataset results and calculated results of both models, with R^2 values of 0.9892 and 0.9997, respectively, which are within acceptable limits.

Overall, the findings indicate that the soft computing methodologies used in this study are quite promising for the cases studied. Artificial intelligence is used to investigate and analyze the complex relationship between soil liquefaction potential, liquefaction-induced settlements caused by liquefaction, and effective liquefaction parameters, which shows a very good ability to understand that correlation in very different ways.

The fundamental drawback of ANFIS modeling is that it cannot provide explicit models or equations for hand calculation. Models of this type rely on database variables to formulate, and their formulation is determined by the data, information, and soil strata used for calibration. Improved prediction over a wider range, additional variables, or soil types would be possible by retraining the model.

References

[1] Zhang G, Robertson PK, Brachman RWI. Estimating liquefaction-induced ground settlements from CPT for level ground. Can Geotech J 2002;39:1168–80. doi:10.1139/t02-047.

[2] Park S-S, Ogunjinmi PD, Woo S-W, Lee D-E. A Simple and Sustainable Prediction Method of Liquefaction-Induced Settlement at Pohang Using an Artificial Neural Network. Sustainability 2020;12:4001. doi:10.3390/su12104001.

[3] Tang X-W, Hu J-L, Qiu J-N. Identifying significant influence factors of seismic soil liquefaction and analyzing their structural relationship. KSCE J Civ Eng 2016;20:2655–63. doi:10.1007/s12205-016-0339-2.

[4] Juwaied NS. APPLICATIONS OF ARTIFICIAL INTELLIGENCE IN GEOTECHNICAL ENGINEERING 2018;13:2764–85.

[5] Park H Il. Study for Application of Artificial Neural Networks in Geotechnical Problems. In: Hui CLP, editor. Artif. Neural Networks, Rijeka: IntechOpen; 2011. doi:10.5772/15011.

[6] Rahman MS, Wang J. Fuzzy neural network models for liquefaction prediction 2002;22:685–94.

[7] Kayadelen C. Expert Systems with Applications Soil liquefaction modeling by Genetic Expression Programming and Neuro-Fuzzy. Expert Syst Appl 2011;38:4080–7. doi:10.1016/j.eswa.2010.09.071.

[8] Ramakrishnan D, Singh TN, Gupta S. Artificial neural network and liquefaction susceptibility assessment : a case study using the 2001 Bhuj earthquake data , Gujarat , India 2012. doi:10.1007/s10596-008-9088-8.

[9] Xue X, Yang X. Application of the adaptive neuro-fuzzy inference system for prediction of soil liquefaction 2013:901–17. doi:10.1007/s11069-013-0615-0.

[10] Ghani S, Kumari S. Evaluation of Liquefaction Based on Hybrid Soft Computing Technique and Conventional Method 2021.

[11] Karkh B, Engineering C, Technology A, Engineering C, Technology A. Neuro-Fuzzy Technique for the Estimation of Liquefaction Potential of Soil 2014;03:617–23.

[12] Sharafi H, Jalili S. Assessment of Cyclic Resistance Ratio (CRR) in Silty Sands Using Artificial Neural Networks 2014:217–28.

[13] Venkatesh K, Kumar V, Tiwari RP. APPRAISAL OF LIQUEFACTION POTENTIAL USING NEURAL NETWORK AND NEURO FUZZY APPROACH 2013;9514. doi:10.1080/08839514.2013.823326.

[14] Idriss IM, Boulanger RW. Semi-empirical procedures for evaluating liquefaction potential during earthquakes 2006;26:115–30. doi:10.1016/j.soildyn.2004.11.023.

[15] Youd T, Hoose S. Historic ground failures in northern California triggered by earthquakes,. 1978.

[16] Youd, T.L., Idriss, I.M., Andrus, R.D., Arango, I., Castro, G., Christian, J.T., Dobry, R., Finn, W.D.L., Harder Jr., L.F. Hynes, M.E., Ishihara, K., Koestor, J.P., Liao, S.S.C., Mar- cuson III, W.F., Martin, G.R., Mitchell, J.K., Moriwaki, Y., Power, M.S KH (2001). Liquefaction Resistance of Soils: Summary Report from the 1996 NCEER and 1998 NCEER/NSF Workshops on Evaluation of Liquefaction Resistance of Soils. J Geotech Geoenvironmental En- Gineering, ASCE, 127(10), 817-833 2001.

[17] Juang CH, Ching J, Wang L, Khoshnevisan S, Ku C-S. Simplified procedure for estimation of liquefaction-induced settlement and site-specific probabilistic settlement exceedance curve using cone penetration test (CPT). Can Geotech J 2013;50:1055–66. doi:10.1139/cgj-2012-0410.

[18] Ishihara K, Yoshimine M. Evaluation of Settlements in Sand Deposits Following Liquefaction During Earthquakes. Soils Found 1992;32:173–88. doi:10.3208/sandf1972.32.173.

[19] Oberhollenzer S, Marte R, Oberhollenzer S, Premstaller M, Marte R. Cone penetration test dataset Premstaller Geotechnik Cone penetration test dataset Premstaller Geotechnik. Data Br 2020;34:106618. doi:10.1016/j.dib.2020.106618.

[20] Ghorbani B, Sadrossadat E, Bolouri Bazaz J, Rahimzadeh Oskooei P. Numerical ANFIS-Based Formulation for Prediction of the Ultimate Axial Load Bearing Capacity of Piles Through CPT Data. Geotech Geol Eng 2018;36:2057–76. doi:10.1007/s10706-018-0445-7.

[21] Jang JSR. ANFIS: Adaptive-Network-Based Fuzzy Inference System. IEEE Trans Syst Man Cybern 1993;23:665–85. doi:10.1109/21.256541.

[22] M. Samhouri , A. Al-Ghandoor , S. Alhaj Ali , I. Hinti WM a. An Intelligent Machine Condition Monitoring System Using Time-Based Analysis: Neuro-Fuzzy Versus Neural Network. Jordan J Mech Ind Eng 2009;3:294–305.

[23] Keshavarz Z, Torkian H. Application of ANN and ANFIS Models in Determining Compressive Strength of Concrete ARTICLE INFO ABSTRACT. J Soft Comput Civ Eng 2018;2:62–70.

[24] Emami H, Emami S. Application of whale optimization algorithm combined with adaptive neuro-fuzzy inference system for estimating suspended sediment load. J Soft Comput Civ Eng 2021;5:1–14. doi:10.22115/SCCE.2021.281972.1300.

[25] Heddam S, Bermad A, Dechemi N. ANFIS-based modelling for coagulant dosage in drinking water treatment plant: a case study. Environ Monit Assess 2012;184:1953–71. doi:10.1007/s10661-011-2091-x.